Supplementary Information

Cytoplasmic pro-apoptotic function of the tumor suppressor p73 is mediated through a modified mode of recognition of the anti-apoptotic regulator Bcl-X_L

Mi-Kyung Yoon[1&], Bu-Yeon Kim[4&], Ji-Young Lee[4], Ji-Hyang Ha[1], Sung Ah Kim[1,3], Dong-Hwa Lee[1], Min-Sung Lee[1,3], Mi-Kyung Lee[1], Jin Sun Choi[1#], Jin Hwa Cho[1], Jeong-Hoon Kim[1,3], Sunhong Kim[1,3], Jaewhan Song[5], Sung Goo Park[1,3], Byoung Chul Park[1,3], Kwang-Hee Bae[2,3], Sang Un Choi[4]* and Seung-Wook Chi[1,3]*

[1]Disease Target Structure Research Center, KRIBB, Daejeon 34141, Republic of Korea, [2]Metabolic Regulation Research Center, KRIBB, Daejeon 34141, Republic of Korea. [3]KRIBB School of Bioscience, Korea University of Science and Technology, Daejeon 34113, Republic of Korea. [4]Bio & Drug Discovery Division, Korea Research Institute of Chemical Technology, Daejeon 34114, Republic of Korea. [5]Department of Biochemistry, Yonsei University, Seoul, Republic of Korea.

Running title: *A modified mode of Bcl-X_L recognition by p73*

[&]These authors contributed equally to this work.

[#]Present address: Research Institute for Medical Sciences, Chungnam National University, Daejeon, Republic of Korea

*To whom correspondence should be addressed: Sang Un Choi; Bio & Drug Discovery Division, Korea Research Institute of Chemical Technology, Daejeon 34114, Republic of Korea; Tel. +82-42-860-7545; Fax. +82-42-861-4246; E-mail: suchoi@krict.re.kr. or Seung-Wook Chi: Disease Target Structure Research Center, KRIBB, Daejeon 34141, Republic of Korea; Tel. +82-42-860-4277; Fax. +82-42-879-8269; E-mail: swchi@kribb.re.kr.

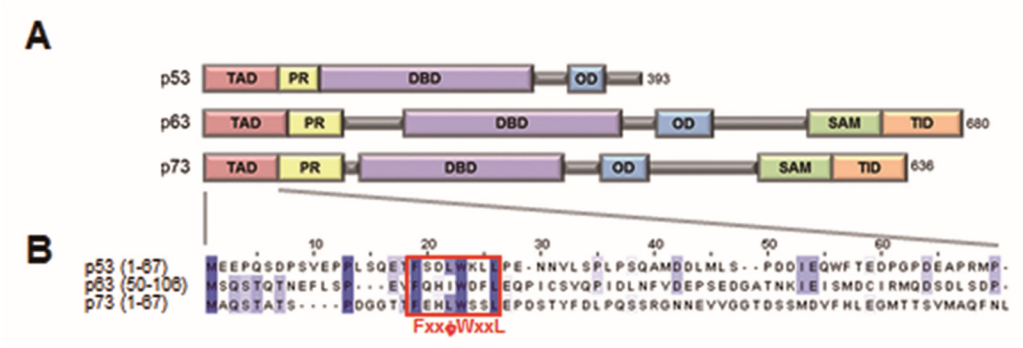

Figure S1. Domain structure of p53 family proteins and sequence alignment of TADs. (A) Domain architecture of the p53 family proteins p53, p63, and p73. TAD, transactivation domain; PR, proline-rich domain; DBD, DNA-binding domain; OD, oligomerization domain; SAM, sterile α-motif; TID, transcription inhibitory domain. (B) The sequence alignment of the TADs of p53, p63, and p73 using ClustalW2. The "FxxΦWxxL" motifs within the TADs, where Φ and x represent a bulky hydrophobic residue and any residue, respectively, are highly homologous and are highlighted with red boxes. The sequences are color-coded based on the sequence identity.

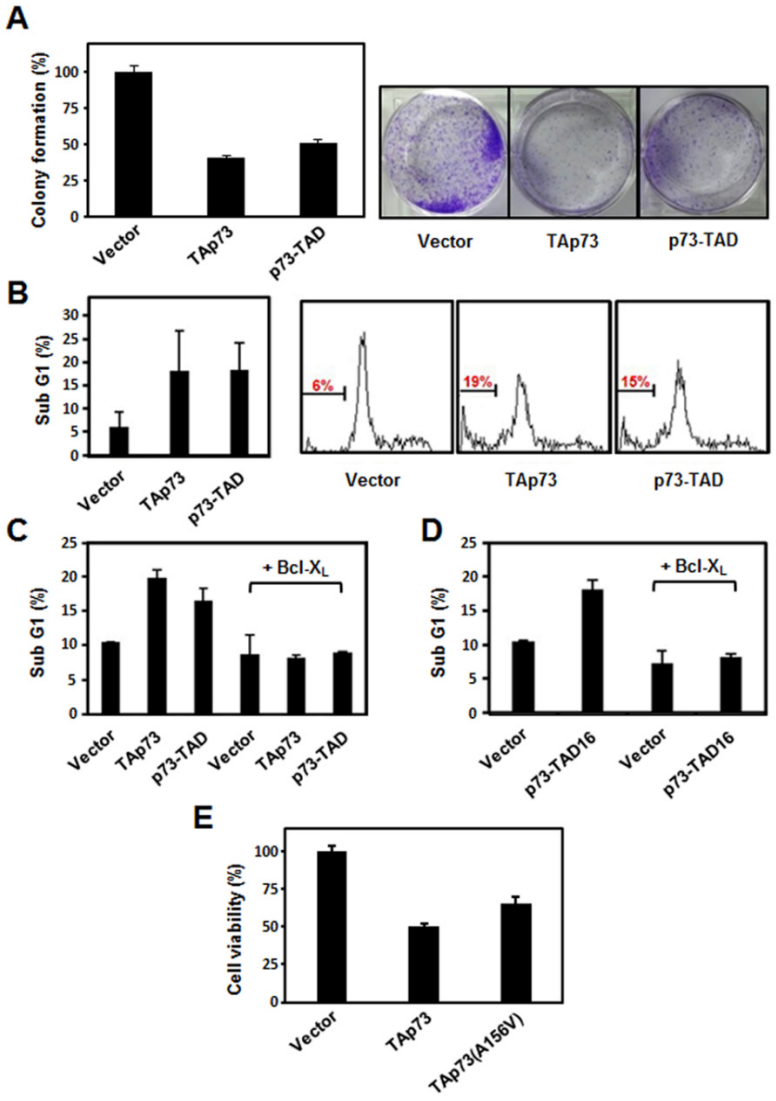

Figure S2. Apoptosis assay with TAp73 and p73-TAD. (A) Colony-formation assay with TAp73 and p73-TAD. TAp73 and p73-TAD suppressed the colony formation of H1299 cells transfected with the indicated plasmids. n=3; $P < 0.001$, compared to control. (B) DNA fragmentation assay with TAp73 and p73-TAD. H1299 cells transfected with the indicated plasmids were stained with DAPI and used for flow cytometric analysis of the DNA content to determine apoptotic cells. n=3; $P < 0.005$, compared to control. (C) The effect of Bcl-X_L on the apoptotic cell death of H1299 cells transfected with peGFP-C3-TAp73 and peGFP-C3-p73-TAD or control vector, as determined by a DNA fragmentation assay. n=3; $P < 0.05$, compared to control. (D) The effect of Bcl-X_L on the apoptotic cell death of H1299 cells transfected with peGFP-C3-TAp73 and peGFP-C3-p73-TAD16, or control vector, as determined by a DNA fragmentation assay. n=3; $P < 0.0001$, compared to control. All data are represented as mean ± s.d. and statistics were performed using one-way ANOVA test. (E) Cell viability assay with a transcriptionally inactive mutant, TAp73(A156V). n=6; $P < 0.0001$, compared to control.

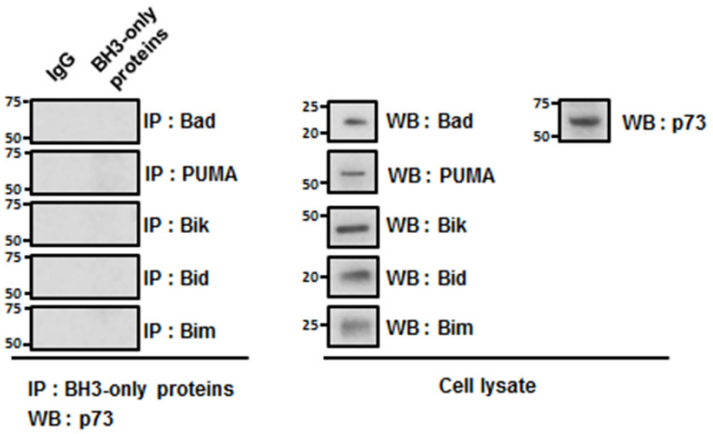

Figure S3. p73 does not bind to pro-apoptotic BH3-only proteins. Endogenous TAp73 does not coimmunoprecipitate with the pro-apoptotic BH3-only proteins Bad, Puma, Bik, Bid, and Bim. Lysates from H1299 cells were immunoprecipitated with the antibodies against the BH3-only proteins and immunoblotted with an anti-p73 antibody.

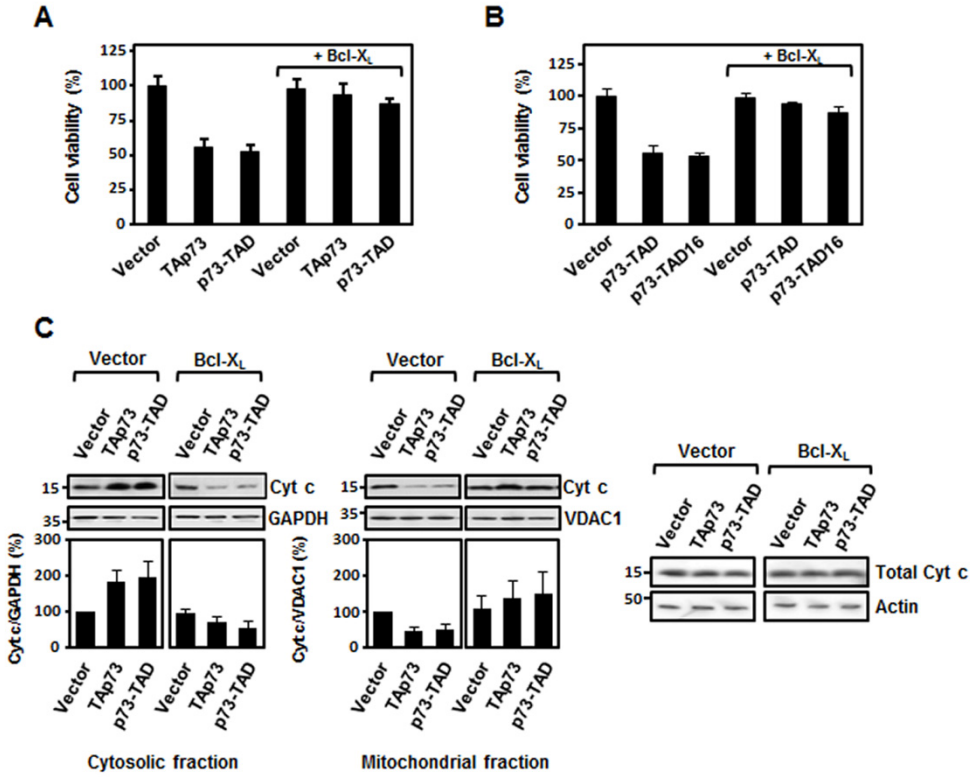

Figure S4. Transcription-independent apoptosis induced by p73-TAD can be blocked by excess Bcl-X_L. (A) Cell viability assays of TAp73 and p73-TAD in the absence and presence of Bcl-X_L. H1299 cells were transfected with peGFP-C3-p73, peGFP-C3-p73-TAD, or peGFP-C3 with or without pCMV2-Flag-Bcl-X_L. peGFP-C3 and pCMV2 were used as controls. After transfection, the cells were treated with DMSO or ActD at 37 °C for 24 h, and then, cell viability was determined using a WST-1 assay. Data points are expressed as fold change relative to vector-transfected cells. n=3; $P < 0.0001$, compared to control. (B) Cell viability of H1299 cells transfected with peGFP-C3-p73-TAD, peGFP-C3-p73-TAD16, or control vector with or without pCMV2-Flag-Bcl-X_L, were analyzed using a WST-1. n=3; $P < 0.0005$, compared to control. (C) Cytochrome c release assay of TAp73 and p73-TAD in the absence and presence of Bcl-X_L. H1299 cells were cotransfected with peGFP-C3-p73 or peGFP-C3-p73-TAD with or without pCMV2-Flag-Bcl-X_L. After subcellular fractionation, the cytosolic and mitochondrial fractions from cell lysates were immunoblotted with an anti-cytochrome c antibody. GAPDH and VDAC1 were used as cytosol and mitochondrial fraction markers, respectively. The graphs in the lower panel represent relative band intensities. Each band intensity was normalized with respect to the GAPDH or VDAC1 band intensity in the same blot. The total amount of cytochrome c is also shown and the experimental time for the cytochrome c release assay is 16 h after transfection. n=4; $P < 0.05$, compared to control. All data are represented as mean ± s.d. and statistics were performed using one-way ANOVA test.

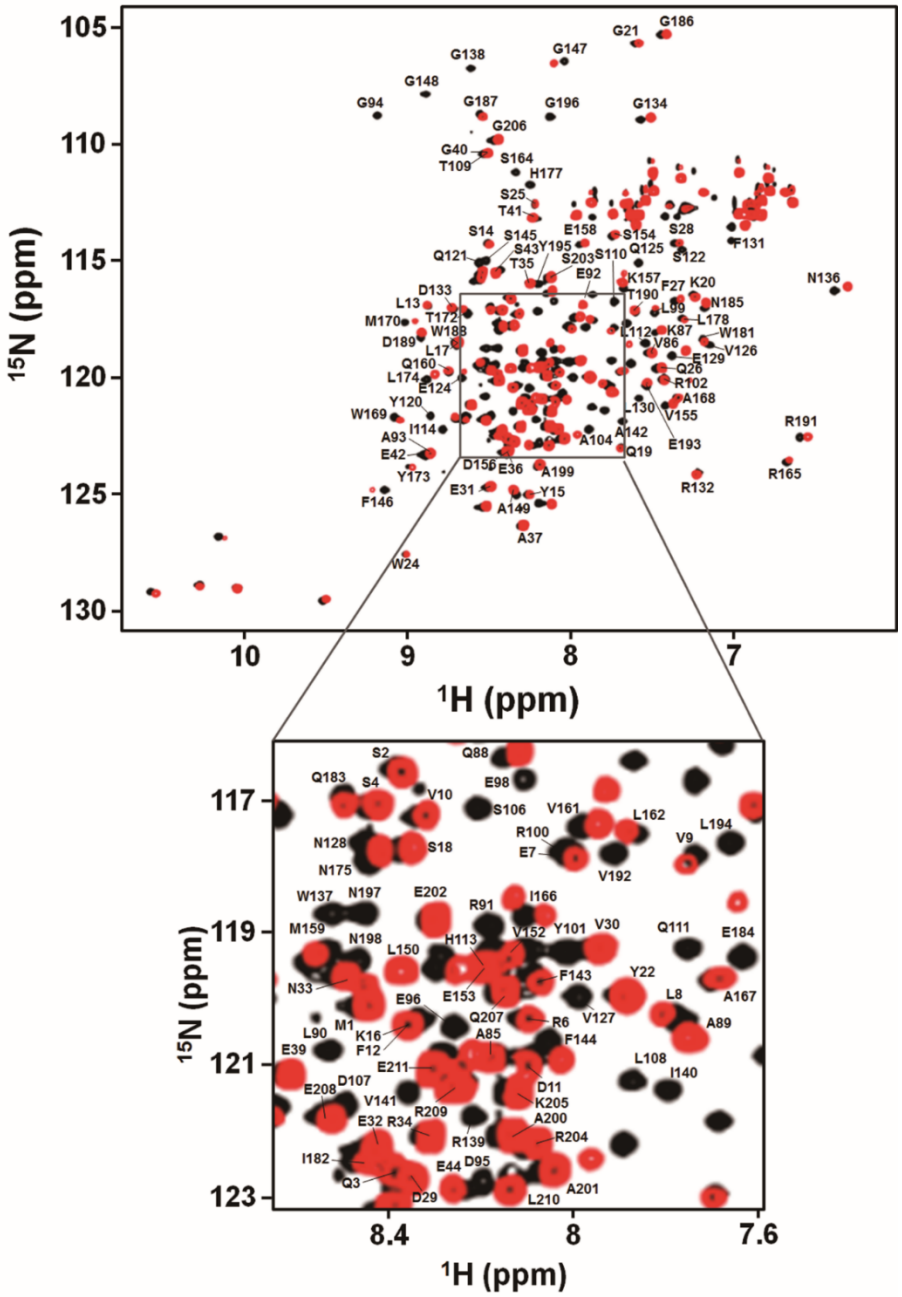

Figure S5. The 2D ^{1}H-^{15}N HSQC spectrum of 1 mM ^{15}N-labeled Bcl-X_L in the absence (black) or presence (red) of 2 mM unlabeled p73-TAD16 peptide. The NMR resonance assignments are labeled.

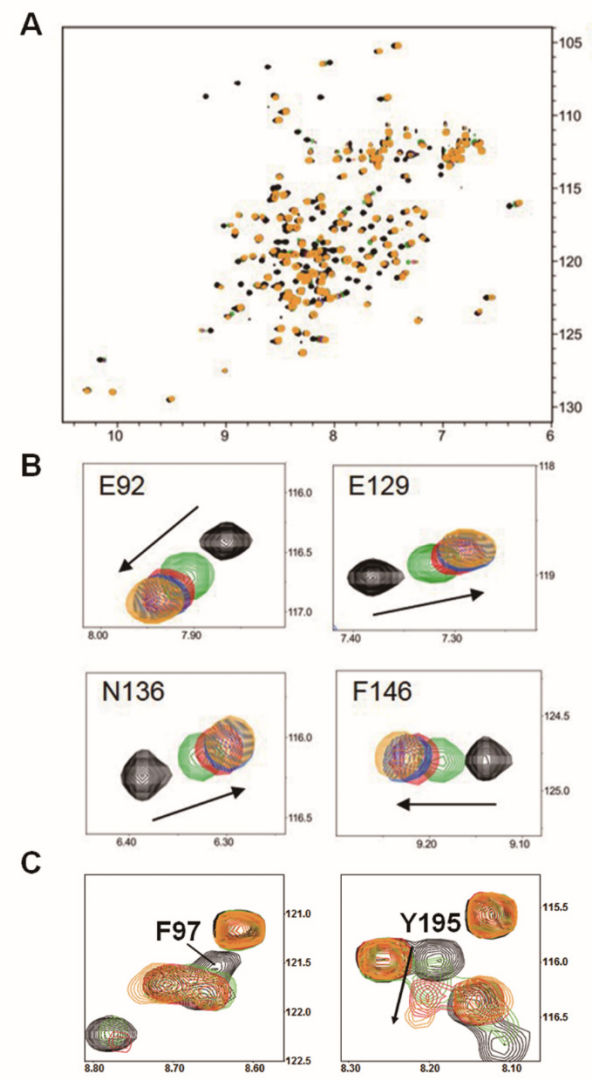

Figure S6. NMR titration analysis of the interaction between Bcl-X_L and the p73-TAD16 peptide. (A) The 2D ^{1}H-^{15}N HSQC spectrum of ^{15}N-labeled Bcl-X_L upon binding to unlabeled p73-TAD16 peptide. (B, C) The NMR chemical shift perturbations of several Bcl-X_L residues upon titration of unlabeled p73-TAD16 peptide to ^{15}N-labeled Bcl-X_L. The chemical shifts of 1 mM (B) or 0.15 mM (C) ^{15}N-Bcl-X_L were monitored upon the addition of unlabeled p73-TAD16 peptide at molar ratios of 1:0 (black), 1:1 (green), 1:2 (red), 1:3 (blue), and 1:4 (orange).

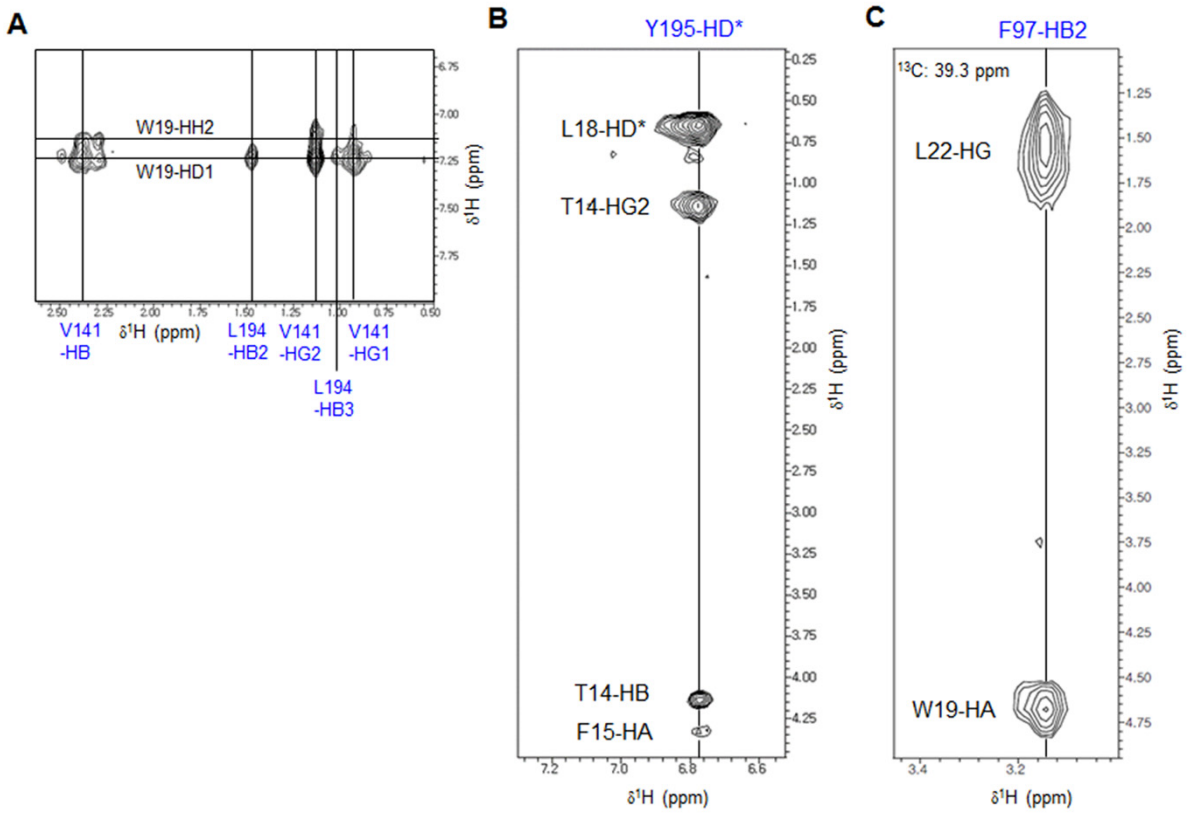

Figure S7. Intermolecular NOE connectivities. 2D (A and B) and 3D (C) versions of the ^{13}C, ^{15}N-filtered, edited NOESY spectra of ^{13}C, ^{15}N-labeled Bcl-X_L bound to the unlabeled p73-TAD16 peptide. Atoms from the Bcl-X_L protein and p73-TAD16 peptide are labeled in blue and black, respectively. Asterisk indicates ambiguous stereospecific assignment.

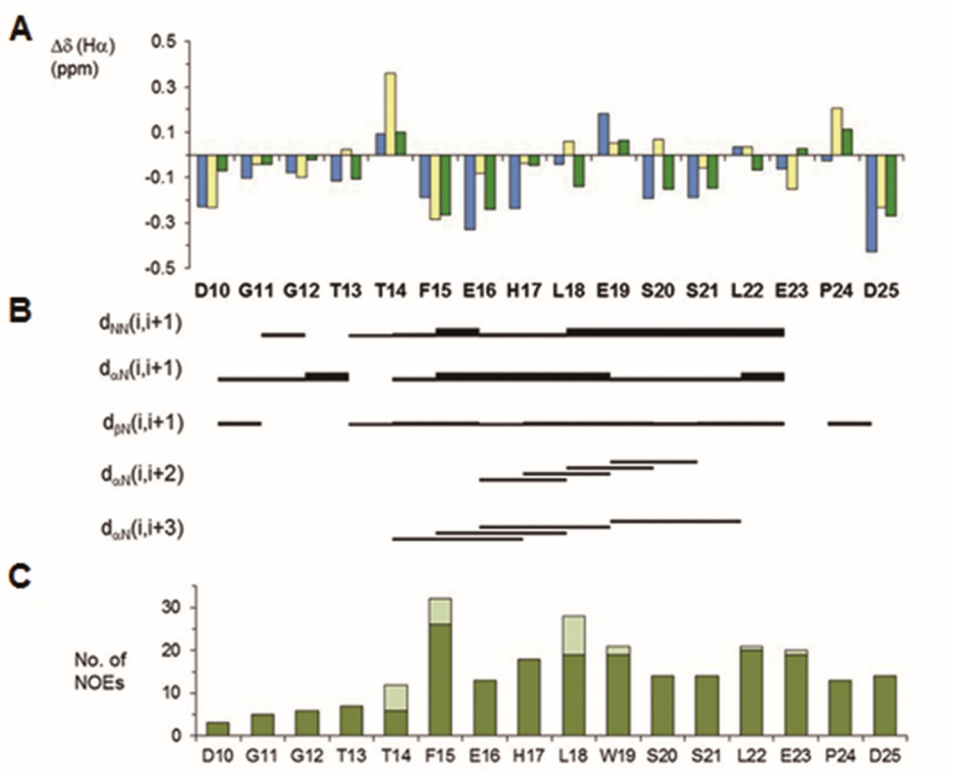

Figure S8. Summary of the secondary structure and NMR distance restraints of the p73-TAD16 peptide. (A) The secondary Hα chemical shifts of the Bcl-X_L-bound p73-TAD16 peptide were derived from the subtraction of three different random coil reference values from the experimental chemical shifts of bound p73-TAD16. The random coil values used were obtained from Schwarzinger et al.(1), Tamiola et al.(2), and Zhang et al.(3) and are shown in blue, yellow, and green, respectively. The bound structural information was obtained from the transferred NOESY of the p73-TAD16 peptide in the presence of Bcl-X_L. (B) The NOE connectivities of p73-TAD16 in the presence of Bcl-X_L. (C) The number of intramolecular (green) and intermolecular (light green) NOEs of the Bcl-X_L-bound p73-TAD16 peptide used in the structure calculation.

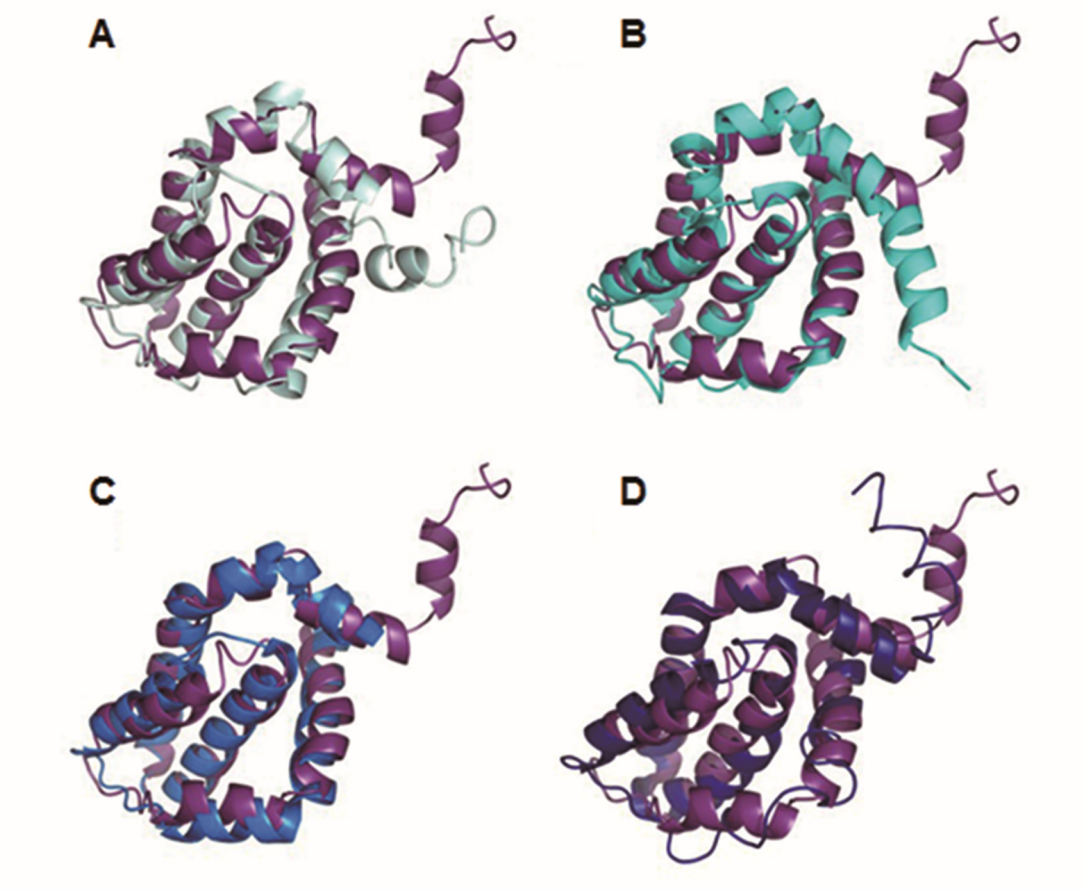

Figure S9. The structural comparisons of p73-TAD16 peptide-bound Bcl-X_L to Bcl-X_L bound to the pro-apoptotic BH3 peptides. (A) The structural comparison of p73-TAD16 peptide-bound Bcl-X_L to Bcl-X_L bound to the pro-apoptotic BH3 peptides of Bak (PDB code: 1BXL). Helix α1, which is not involved in any peptide binding, and pro-apoptotic BH3 peptides are not shown for clarity. The Bcl-X_L protein bound to the p73-TAD16 peptide is colored purple, and the Bcl-X_L proteins bound to pro-apoptotic BH3 peptides are colored from light to dark blue. (B) The structural comparison of p73-TAD16 peptide-bound Bcl-X_L to Bcl-X_L bound to the pro-apoptotic BH3 peptides of Bad (PDB code: 1G5J). (C) The structural comparison of p73-TAD16 peptide-bound Bcl-X_L to Bcl-X_L bound to the pro-apoptotic BH3 peptides of Bim (PDB code: 3FDL). (D) The structural comparison of p73-TAD16 peptide-bound Bcl-X_L to Bcl-X_L bound to the pro-apoptotic BH3 peptides of PUMA (PDB code: 2M04).

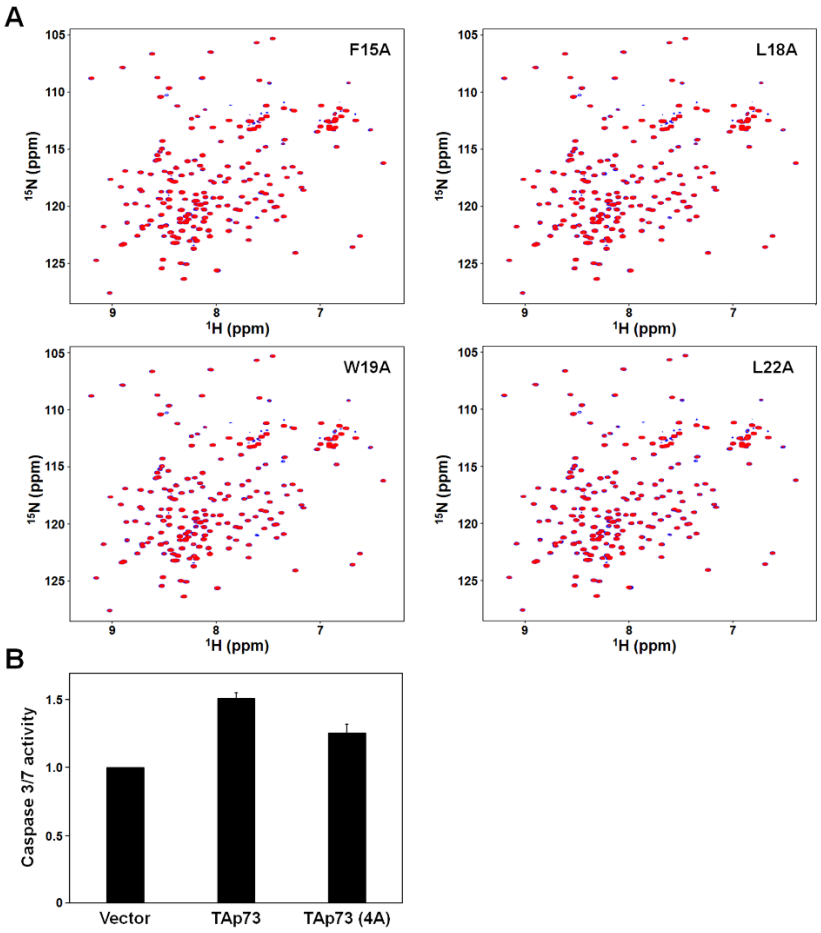

Figure S10. Mutational study on the interaction between Bcl-X_L and p73-TAD16. (A) NMR experiments for Bcl-X_L binding using mutant p73-TAD16 peptides. The overlaid 2D ^{1}H-^{15}N HSQC spectra of ^{15}N-labeled Bcl-X_L in the absence (blue) and presence (red) of mutant p73 peptides containing F15A, L18A, W19A, or L22A. (B) Caspase-3/7 activity with TAp73(4A) mutant. Caspase-3/7 activity was measured in H1299 cells transfected with peGFP-C3-TAp73(4A) mutant or peGFP-C3-TAp73. n=3; $P < 0.005$, compared to control. Data are represented as mean ± s.d.

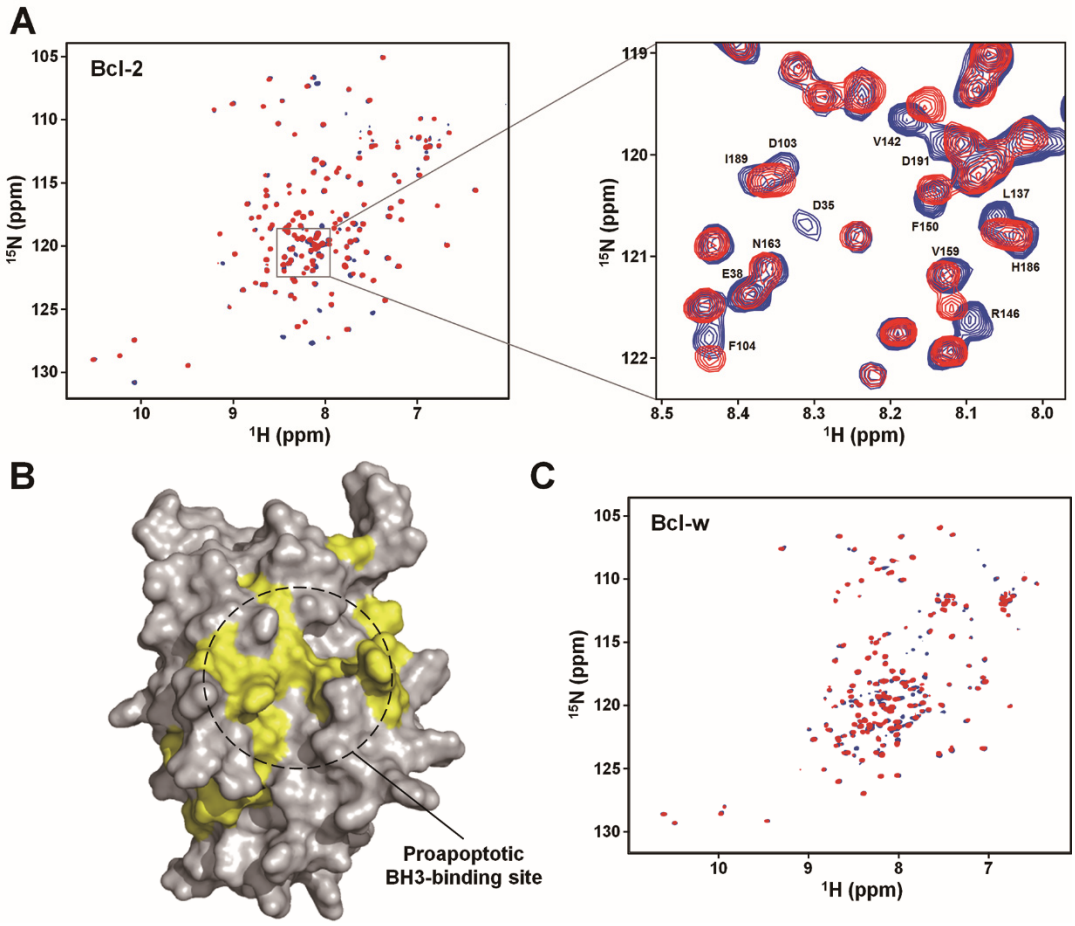

Figure S11. NMR experiments for binding of Bcl-2 or Bcl-w with the p73TAD-16 peptide. (A) The 2D ^{1}H-^{15}N HSQC spectrum of ^{15}N-labeled Bcl-2 in the absence (blue) or presence (red) of the unlabeled p73-TAD16 peptide. (B) Binding site mapping of the p73TAD16 peptide on the Bcl-2 structure by NMR. The chemical shift perturbations are shown in yellow. The pro-apoptotic BH3 peptide-binding site is indicated. (C) The 2D ^{1}H-^{15}N HSQC spectrum of ^{15}N-labeled Bcl-w in the absence (blue) or presence (red) of the unlabeled p73-TAD16 peptide. The chemical shifts of 0.1 mM ^{15}N-Bcl-2 or 0.1 mM ^{15}N-Bcl-w were monitored upon addition of the unlabeled p73-TAD16 peptide at the molar ratio of 1:4.

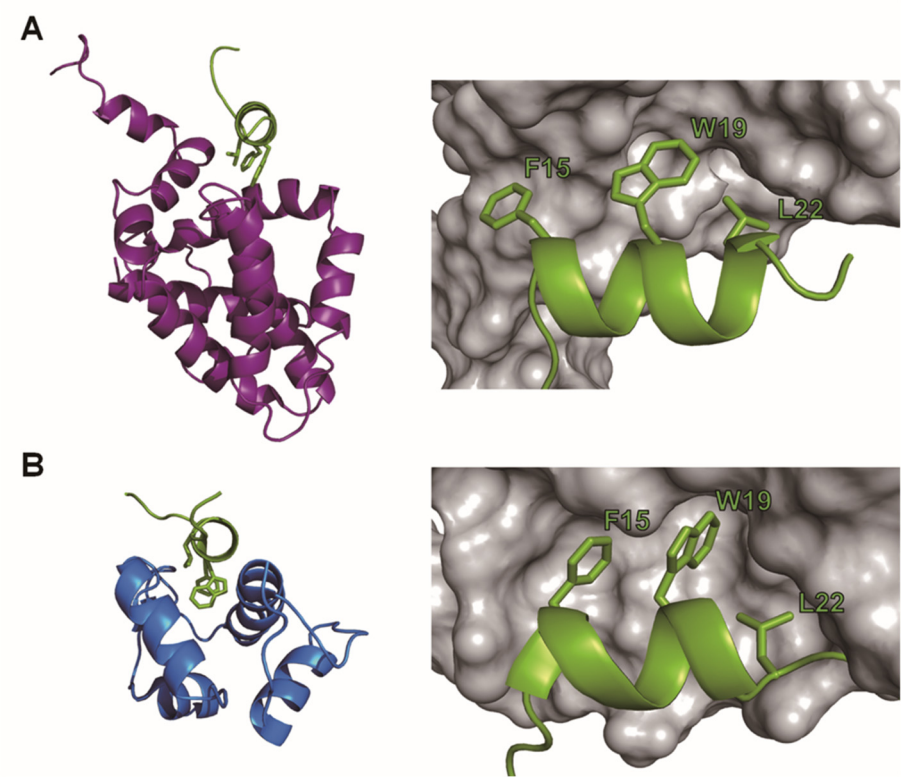

Figure S12. Mimicry in the recognition of Bcl-X_L and MDM2 by the p73-TAD16 peptide. (A) Structure of the Bcl-X_L/p73-TAD16 peptide complex. The p73-TAD16 peptides are drawn as light green ribbon models, and the critical binding determinants of the peptide for Bcl-X_L are labeled. (B) Structure of MDM2/p73-TAD16 peptide complex (PDB code: 6IJQ).

References

1. Schwarzinger, S., Kroon, G. J., Foss, T. R., Chung, J., Wright, P. E., and Dyson, H. J. (2001) Sequence-dependent correction of random coil NMR chemical shifts. *J Am Chem Soc* **123**, 2970-2978
2. Tamiola, K., Acar, B., and Mulder, F. A. (2010) Sequence-specific random coil chemical shifts of intrinsically disordered proteins. *J Am Chem Soc* **132**, 18000-18003
3. Zhang, H., Neal, S., and Wishart, D. S. (2003) RefDB: a database of uniformly referenced protein chemical shifts. *J Biomol NMR* **25**, 173-195